JOURNAL OF VIROLOGY, Apr. 2011, p. 3557–3569 Vol. 85, No. 7
0022-538X/11/$12.00 doi:10.1128/JVI.01191-10

N1L Is an Ectromelia Virus Virulence Factor and Essential for *In Vivo* Spread upon Respiratory Infection▽

Meike S. Gratz,[1] Yasemin Suezer,[1] Melanie Kremer,[2] Asisa Volz,[2] Monir Majzoub,[4] Kay-Martin Hanschmann,[1] Ulrich Kalinke,[1,3] Astrid Schwantes,[1] and Gerd Sutter[1,2]*

Paul-Ehrlich-Institut, Langen, Germany[1]; Institute for Infectious Diseases and Zoonoses, Ludwig-Maximilians-Universität München, Munich, Germany[2]; TWINCORE, Center for Experimental and Clinical Infection Research, Hannover, Germany[3]; and Institute of Veterinary Pathology, Ludwig-Maximilians-Universität München, Munich, Germany[4]

Received 3 June 2010/Accepted 30 December 2010

The emergence of zoonotic orthopoxvirus infections and the threat of possible intentional release of pathogenic orthopoxviruses have stimulated renewed interest in understanding orthopoxvirus infections and the resulting diseases. Ectromelia virus (ECTV), the causative agent of mousepox, offers an excellent model system to study an orthopoxvirus infection in its natural host. Here, we investigated the role of the vaccinia virus ortholog N1L in ECTV infection. Respiratory infection of mice with an N1L deletion mutant virus (ECTVΔN1L) demonstrated profound attenuation of the mutant virus, confirming N1 as an orthopoxvirus virulence factor. Upon analysis of virus dissemination *in vivo*, we observed a striking deficiency of ECTVΔN1L spreading from the lungs to the livers or spleens of infected mice. Investigating the immunological mechanism controlling ECTVΔN1L infection, we found the attenuated phenotype to be unaltered in mice deficient in Toll-like receptor (TLR) or RIG-I-like RNA helicase (RLH) signaling as well as in those missing the type I interferon receptor or lacking B cells. However, in RAG-1$^{-/-}$ mice lacking mature B and T cells, ECTVΔN1L regained virulence, as shown by increasing morbidity and virus spread to the liver and spleen. Moreover, T cell depletion experiments revealed that ECTVΔN1L attenuation was reversed only by removing both CD4$^+$ and CD8$^+$ T cells, so the presence of either cell subset was still sufficient to control the infection. Thus, the orthopoxvirus virulence factor N1 may allow efficient ECTV infection in mice by interfering with host T cell function.

In 1980, the World Health Organization (WHO) announced the successful eradication of human smallpox and elimination of its causative agent, the highly pathogenic variola virus (VARV) (24). This achievement resulted in cessation of vaccination. As a consequence, immunity to orthopoxviruses within the human population has greatly declined. Today, the risk of intentionally released pathogenic orthopoxviruses and the more frequent appearance of zoonotic diseases in humans, caused by infections with cowpox or monkeypox viruses, pose new challenges to our public health systems, as well as renewed interest in the study of orthopoxvirus infections and the resulting diseases (10, 17, 19, 57).

Host-specialized orthopoxviruses, such as VARV and ectromelia virus (ECTV), infect with high efficiency, spread systemically within their hosts, and are effectively transmitted to others. Such efficient replication and spreading relies on highly adapted viral interference with the host immune system, presumably at multiple levels. This hypothesis is well supported by the fact that orthopoxviruses encode many host regulatory proteins with the potential to serve as immune evasion factors (1, 20, 26, 35, 59, 62, 63, 66). These so-called host response modifiers include soluble decoy receptors of inflammatory cytokines and chemokines (6, 13, 44, 64) as well as inhibitors of intracellular signaling pathways, such as those of Toll-like receptor (TLR) signaling (7). Other factors interfere with the induction of apoptosis, e.g., the proteins p28, F1, and E3 (11, 27, 28, 72).

The regulatory protein N1 encoded by the N1L gene of vaccinia virus (VACV) strain Western Reserve (VACV WR) was found to be a strong virulence factor upon *in vivo* infection of mice (3, 40). In the intracranial infection model in BALB/c mice, virulence of the N1L deletion mutant virus was greatly reduced, and the virus was also reported to be attenuated in intraperitoneally (i.p.) infected athymic nude mice (40). Upon intranasal infection of C57BL/6 mice, the virus lacking the N1L gene induced less weight loss and morbidity, and lesion size and viral load were reduced following intradermal inoculation in the ear pinna model (3). However, the mechanisms responsible for the attenuation of the VACV N1L deletion mutant virus are not known to date. The N1L open reading frame (ORF) encodes a protein of approximately 14 kDa, which is expressed early during infection (3, 40). N1 is located predominantly within the cell (3) and shows structural similarity to members of the Bcl-2 family of pro- and antiapoptotic proteins (2, 14). It was additionally reported to interfere with NF-κB signaling at the IKK complex (18) and to inhibit staurosporine-induced apoptosis (14).

So far, N1 has been reviewed only in the VACV background, for which the natural host organism is not yet known. Thus, in this study, we decided to analyze N1L function in ECTV, the causative agent of mousepox (20), to make use of a natural virus-host system. We investigated the pathogenesis of the mutant virus ECTVΔN1L and its interaction with the host immune response. The gene homologous to VACV N1L was

* Corresponding author. Mailing address: Institute for Infectious Diseases and Zoonoses, Faculty of Veterinary Medicine, LMU Munich, Veterinärstr. 13, 80539 Munich, Germany. Phone: 49 89 2180 2610. Fax: 49 89 2180 16576. E-mail: gerd.sutter@lmu.de.

▽ Published ahead of print on 26 January 2011.

deleted from the ECTV genome (ORF 020), and the resulting mutant virus was attenuated *in vivo*. Interestingly, it failed to spread to internal organs after respiratory infection of mice, although replication in tissue culture was unaffected. In a characterization of the ECTVΔN1L infection in various mouse models with immune deficiencies, we revealed that the presence of either $CD4^+$ or $CD8^+$ T cells was essential to maintain attenuation and therefore to control ECTVΔN1L infection.

MATERIALS AND METHODS

Cells and viruses. Monolayers of BS-C-1 (ATCC CCL-26) and NIH 3T3 (ATCC CRL-1658) cells were cultivated in Dulbecco's modified Eagle's medium (DMEM; Biochrom AG, Berlin, Germany), supplemented with 10% heat-inactivated fetal calf serum (FCS; Biochrom AG, Berlin, Germany), 1% L-glutamine, and 1% penicillin/streptomycin (Biochrom AG, Berlin, Germany). All cells were maintained at 37°C, with 5% CO_2, and at 90% relative humidity.

Ectromelia virus (ECTV) strain Moscow (EMBL-EBI accession number AF012825) was a kind gift from R. Mark L. Buller (St. Louis University School of Medicine, St. Louis, MO). All viruses were routinely propagated on BS-C-1 cells, and titers were determined by plaque assays on BS-C-1 cells (see the analysis of viral growth). Briefly, confluent BS-C-1 cells were infected, and after 3 days, cells and supernatants were harvested and subjected to three cycles of freezing and thawing. For *in vivo* stock viruses, the virus preparation was centrifuged at 1,000 × *g* to remove large cell debris. High-titer virus stocks for *in vitro* infections were prepared by ultracentrifugation. In a first step, virus particles were pelleted, and the pellet was resuspended in 10 mM Tris-HCl (pH 8.0). Following another three cycles of freezing and thawing as well as sonication, the virus preparation was purified by ultracentrifugation through a sucrose cushion (36% [wt/vol] sucrose in 10 mM Tris-HCl [pH 8.0]). Finally, the pellet was resuspended in 10 mM Tris-HCl (pH 8.0). Prior to infection, all virus preparations were sonicated three times.

Construction of ECTVΔN1L and ECTV-N1Lrev. For the construction of recombinant viruses, the plasmid pUC18*-gpt-lacZ served as a basis to generate other plasmids. Initially, most of the existing *lacZ* gene sequence in the plasmid pUC18 (Invitrogen, Darmstadt, Germany) was deleted by enzymatic restriction with NdeI and HindIII. The resulting pUC18* was then treated with Klenow fragment (New England BioLabs, Frankfurt am Main, Germany) to generate blunt ends. Subsequently, the *gpt-lacZ* cassette (65), excised from pcDNA3.1-gpt-lacZ using PstI, was inserted into PstI-restricted pUC18* to form the plasmid pUC18*-gpt-lacZ.

The plasmid pΔN1L, used to create ECTVΔN1L, was generated by splicing by overlap extension (SOE) PCR as described previously (32). Sequences flanking the N1L ORF were amplified by PCR from genomic ECTV DNA using primer pair P1 (5′-AAAGTCGACGCTCTTATTCTGTACGAATC-3′) and P2 (5′-**CTTATCAGTAGGATGA**TTGAAAAGTATTT-3′) and primer pair P3 (5′-**TCATCCTACTGATAAG**TAGAGTCCTC-3′) and P4 (5′-AAACCCGGGTGCCATATTGGATAGATTCC-3′). Primers P1 and P4 contained restriction sites specific for SalI and XmaI, respectively (underlined). The amplified sequences were fused in a third PCR using primers P1 and P4, with nucleotides depicted in bold in P2 and P3 marking overlapping parts that facilitated the fusion. The resulting amplicon was treated with SalI and XmaI and cloned into pUC18*-gpt-lacZ.

Similarly, the sequence of the N1L gene with flanking sequences was amplified by PCR using primers P1 and P4. Again, the amplicon was treated with SalI and XmaI and cloned into pUC18*-gpt-lacZ to form the plasmid pN1Lrev.

All plasmids were sequenced following completion of the cloning procedure to confirm their sequence integrity.

The two recombinant viruses, ECTVΔN1L and ECTV-N1Lrev, were generated by transient dominant selection (TDS) using the *Escherichia coli gpt* gene as a selection marker, as described previously (8, 21). Briefly, confluent BS-C-1 monolayers seeded in six-well plates were infected with the ECTV wild type (wt) at a multiplicity of infection (MOI) of 0.5. After 1.5 h, cells were transfected with 4 μg of pΔN1L plasmid DNA using Lipofectamine 2000 (Invitrogen, Darmstadt, Germany) according to the manufacturer's instructions. Following incubation for 2 to 3 days, samples were harvested, and the recombinant virus was plaque purified as described previously (21, 45). The revertant virus, ECTV-N1Lrev, was generated accordingly, using ECTVΔN1L and the plasmid pN1L-rev for infection and transfection, respectively.

Analysis of viral growth. For one-step and multiple-step growth curves, approximately 80% confluent monolayers of BS-C-1 and NIH 3T3 cells were infected at an MOI of 10 and 0.01, respectively. After a 1-hour incubation step at 37°C, the cells were washed three times with phosphate-buffered saline (PBS) before fresh medium with 2% FCS was added. Cells and supernatants were harvested at 0, 4, 8, 12, 24, and 48 h postinfection (p.i.) for the one-step analysis and at 0, 12, 24, 48, and 72 h p.i. for the multiple-step analysis. Samples were subjected to three cycles of freezing and thawing, and viral titers were determined by plaque assays on BS-C-1 cells as described previously (41). Briefly, samples were sonicated three times, and serial dilutions were plated in duplicate onto confluent BS-C-1 cells in six-well plates. The medium was changed 2 h later. After 48 h, cells were fixed and stained with crystal violet solution (0.01% in 20% ethanol). Subsequently, the plaques were counted.

Analysis of N1L expression. To monitor expression of N1L, confluent BS-C-1 cells in six-well plates were infected at an MOI of 5. The virus was allowed to adsorb to cells for 30 min at 4°C before medium was replaced by fresh infection medium (2% FCS). At 24 h p.i., samples were prepared by lysing the cells with radioimmunoprecipitation assay (RIPA) lysing buffer (25 mM Tris-HCl [pH 8], 137 mM sodium chloride, 2 mM EDTA, 1% glycerol, 1% NP-40, 0.5% sodium deoxycholate, 0.1% sodium dodecyl sulfate [SDS]) supplemented with a protease inhibitor cocktail (Complete; Roche Diagnostics, Mannheim, Germany). Lysates were cleared using QIAshredder columns (Qiagen, Hilden, Germany), separated by SDS-polyacrylamide gel electrophoresis (SDS-PAGE) with 12% polyacrylamide gels, and blotted onto nitrocellulose membranes (Bio-Rad, Munich, Germany). Following a blocking step, the N1 protein was detected using an N1-specific rabbit antiserum (see below) as the primary antibody, a secondary goat anti-rabbit peroxidase-coupled antibody (Dianova, Hamburg, Germany), and enhanced chemiluminescence (ECL) substrate (Amersham, Freiburg, Germany). The rabbit polyclonal antiserum specific for the N1 was used at a 1:200 dilution.

Generation of an N1-specific rabbit-antiserum. A polyclonal antibody directed against the N1 protein was raised by immunization of rabbits with two peptides (H2N-CMR MTL SDG PLL DRL-CONH2 and H2N-CKV ARD IGE RSE IR-CONH2), which were derived from the VACV N1 protein (Eurogentec, Seraing, Belgium) and which corresponded to peptide sequences in the ECTV N1 protein.

Mice. Female C57BL/6N mice (6 to 8 weeks old) were purchased from Charles River Laboratories (Sulzfeld, Germany). C57BL/6J-$Rag1^{tm1Mom}$ (recombination-activating gene 1 deficient [$RAG\text{-}1^{-/-}$]) (50), B6.129S7-*Ifnar1tm1Agt* (type I interferon receptor deficient [$IFNAR^{-/-}$]) (52), $MyD88^{-/-}$ $TRIF^{-/-}$ (C57BL/6 background) (70, 73), $Cardif^{-/-}$ (C57BL/6 background) (42), and JHT (C57BL/6 background) (29) mice were bred under specific-pathogen-free conditions at the central animal facility of the Paul-Ehrlich-Institut. For experimental work, mice were housed in an ISOcage unit (Tecniplast, Hohenpeissenberg, Germany) and had free access to food and water. All animal experiments were approved by the Government of the State of Hesse (Germany), and animals were handled in compliance with German regulations for animal experimentation (Animal Welfare Act).

Intranasal infection of mice. Mice were anesthetized by i.p. injection of 10 mg/ml of ketamine and 0.4 mg/ml of xylazine applied at 0.1 ml per 10 g of body weight. The virus suspension in a total volume of 30 μl or virus-free medium (control) was instilled equally into both nostrils. Changes in weight and signs of illness were monitored daily.

Depletion of specific cell populations in mice. Mice were depleted of specific immune cell populations by i.p. administration of mouse monoclonal antibodies. To deplete NK cells, mice were given 300 μg of anti-NK1.1 antibody PK136 (Harlan Bioproducts, Indianapolis, IN) i.p. on days 2 and 1 prior to infection. Additionally, animals were given a boost on day 12 p.i. Single T cell subsets were depleted using the monoclonal antibodies anti-CD4 GK1.5 and anti-CD8 2.43 (both Harlan Bioproducts, Indianapolis, IN). Mice were given 500 μg of anti-CD4 GK1.5 i.p. on days 8, 6, 3, 2, and 1 prior to infection, while 100 μg of anti-CD8 2.43 was administered on days 2 and 1 prior to infection. For both antibodies, animals were given a boost on day 12 p.i. Depletion of both $CD4^+$ and $CD8^+$ T cell subsets was achieved by combining the two application schemes.

Determination of viral load in mouse organs and histopathology. Organs were removed either at the indicated time points (see Fig. 3, 5, and 8) or when animals died due to infection or had to be sacrificed during or at the end of an experiment. Up to 0.2 g of organ in 1 ml PBS was homogenized in Lysing Matrix A tubes using FastPrep-24 (40 s, level 6.0) from MP Biomedicals (Illkirch, France). Tubes were chilled on ice for 5 min and then centrifuged for 5 min at 14,000 × *g* and 4°C. Supernatants were stored at −80°C until titration (see analysis of viral growth).

For histopathologic examination of the lung and liver, C57BL/6 mice were infected intranasally with 200 PFU of the ECTV wt, ECTVΔN1L, or ECTV-N1Lrev. On day 6 p.i., mice were sacrificed. The lungs (inflated) and livers were removed, fixed in phosphate-buffered formalin, and embedded in paraffin. Sec-

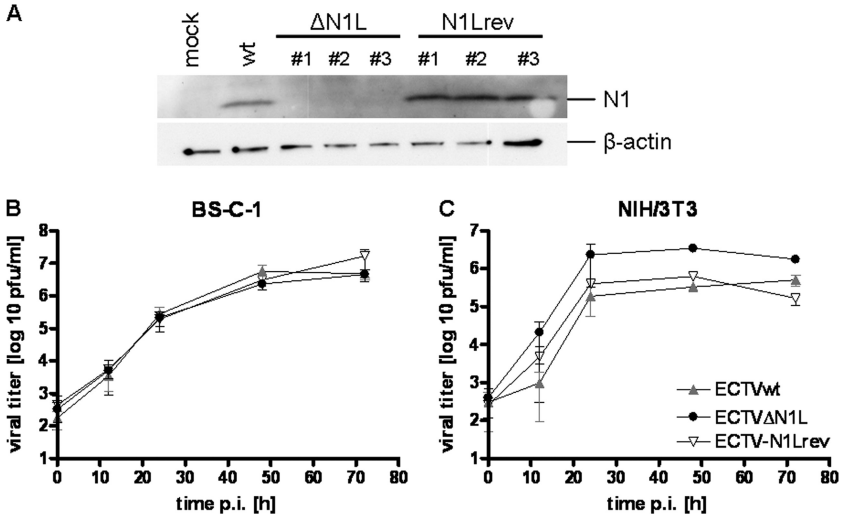

FIG. 1. Analysis of N1L expression and viral growth. (A) Synthesis of N1 protein was assessed in BS-C-1 cells infected with ECTV wt (wt) or one of three clonal isolates of ECTVΔN1L (ΔN1L #1 to #3) or ECTV-N1Lrev (N1Lrev #1 to #3) at 24 h p.i. (MOI, 5). Mock-infected cells (mock) served as a control. Cell lysates were prepared and separated in a 12% SDS-polyacrylamide gel. After the proteins were transferred to nitrocellulose membranes, the N1 protein and β-actin were detected using an N1-specific polyclonal rabbit antiserum and β-actin-specific monoclonal mouse antibody, respectively. (B and C) Multiple-step growth analysis of ECTV wt, ECTVΔN1L, or ECTV-N1Lrev was performed with BS-C-1 (B) and NIH 3T3 (C) cells infected at an MOI of 0.01. Data shown are mean values from two or three independent experiments.

tions (4 μm) were stained with hematoxylin and eosin before being examined by light microscopy.

Statistical analysis. Statistical comparison of *in vitro* growth curves in BS-C-1 and NIH 3T3 cells was performed by one-factorial analysis of variance (ANOVA) for the area under the log titer curves (AUC). The progression of disease following intranasal infection of C57BL/6 mice and different knockout mouse strains was analyzed by one-factorial ANOVA for the area under the percentage of initial weight curves. For survival data, Kaplan-Meyer curves were calculated and compared by means of a log-rank test. The viral loads in the lungs (see Fig. 5A) were compared by one-factorial ANOVA for log titers (separately for each day). For multiple comparisons, *P* values and confidence intervals were adjusted according to the method of Bonferroni (see Fig. 1B and C, 2A, 6A to C, and 7A to C) or Dunnett-Hsu (see Fig. 2C, 5A, and 9A to D) in order to control for overall type I error. All statistical analyses were performed with SigmaPlot software (version 8; Systat) and SAS/STAT software (version 9.2; SAS system for Windows).

RESULTS

ECTV Moscow N1L homolog is dispensable for viral replication and cell-to-cell spread *in vitro*. To study the function of N1L in ECTV, we deleted ORF 020, corresponding to the VACV N1L gene, from the ECTV genome to generate ECTVΔN1L. The deletion mutant was constructed by removing approximately 80% of the ECTV 020 coding sequence, as described previously for N1L in VACV (3), using the method of transient dominant selection (21). The corresponding revertant virus, ECTV-N1Lrev, was subsequently generated by reinserting the deleted ECTV 020 sequence into its original locus, resulting in N1L gene expression under transcriptional control of its authentic promoter.

To confirm the inactivation of N1L gene expression in ECTVΔN1L, we monitored synthesis of the N1 protein in BS-C-1 cells infected with the ECTV wt, ECTVΔN1L, or ECTV-N1Lrev for 24 h (Fig. 1A). As expected, Western blot analysis revealed N1 proteins in lysates from cells infected with ECTV wt or either of three different clonal isolates of ECTV-N1Lrev, whereas no N1 protein was detected upon ECTVΔN1L infection (Fig. 1A, upper panel). For all subsequent experiments, the clonal isolate ECTVΔN1L1 and the revertant virus derived thereof, ECTV-N1Lrev1, were used.

Next, we analyzed the growth behavior of ECTVΔN1L *in vitro*. Multiple-step growth analyses were performed with BS-C-1 cells, which are routinely used for propagating ECTV, and with NIH 3T3 cells to assess the replicative capacity of ECTVΔN1L in cells of murine origin. In both cell lines, the growth of ECTVΔN1L and ECTV-N1Lrev was comparable to that of the ECTV wt: the three viruses replicated to similar titers within 72 h, each covering a range of approximately three log steps in BS-C-1 cells (Fig. 1B) (*P* value of 1.0 comparing the ECTV wt and ECTVΔN1L, *P* value of 0.8902 comparing ECTV wt and ECTV-N1Lrev, *P* value of 0.9818 comparing ECTVΔN1L and ECTV-N1Lrev) and four in NIH 3T3 cells (Fig. 1C) (*P* value of 1.0 for all comparisons). Similar results were obtained with one-step growth analyses (data not shown), indicating that N1L does not seem to influence ECTV replication.

ECTVΔN1L is highly attenuated after respiratory infection of mice. To assess whether the N1 protein contributes to ECTV virulence, we tested ECTVΔN1L in a mouse model of respiratory infection. C57BL/6 mice were infected intranasally with 200 PFU of the ECTV wt, ECTVΔN1L, or ECTV-N1Lrev and then monitored daily for weight loss, signs of illness, and mortality. Mice infected with the ECTV wt showed morbidity and mortality profiles matching those previously described (54) (Fig. 2A and B), with a mean time to death (MTTD) of 10.5 days. Although three out of six animals survived the ECTV-N1Lrev infection (Fig. 2B), all mice in this group lost up to 25% of their initial body weight (Fig. 2A), indicating a disease progression very similar to that observed for ECTV wt-infected animals (MTTD of 11.3 days). In contrast, all mice infected with ECTVΔN1L survived (Fig. 2B) (*P* value of 0.0012 compared to the ECTV wt) and, more strikingly, neither lost

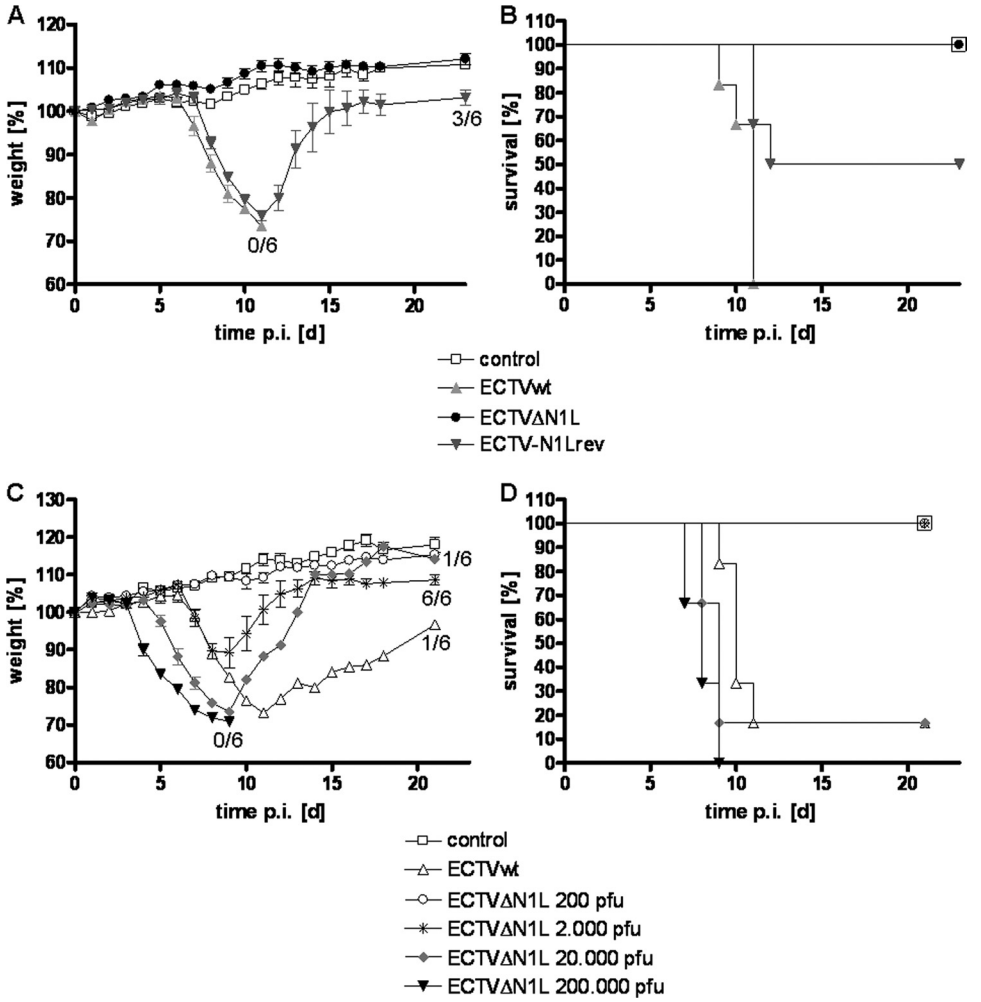

FIG. 2. Morbidity and mortality of C57BL/6 mice infected intranasally with ECTVΔN1L. (A and B) Groups of four to six C57BL/6 mice were mock infected or infected intranasally with 200 PFU of the ECTV wt, ECTVΔN1L, or ECTV-N1Lrev. Mice were monitored daily for up to 23 days p.i. for weight changes. (A) Weight is expressed as percent initial body weight at the day of infection. Additionally, the number of animals that survived the infection of the total number of animals per group is indicated for selected groups. (B) Survival of mice was plotted in a Kaplan-Meyer survival curve. (C and D) Groups of four to six C57BL/6 mice were mock infected or infected intranasally with 200 PFU of ECTV wt or with increasing doses of ECTVΔN1L (2,000 PFU to 200,000 PFU). Mice were monitored daily for up to 21 days p.i. for weight changes. (C) Weight is expressed as percent initial body weight at the day of infection. Additionally, the number of animals that survived the infection of the total number of animals per group is indicated for selected groups. (D) Survival of mice was plotted in a Kaplan-Meyer survival curve. The standard deviation (B and D) is given as the standard error of the mean (SEM). Data are representative of results of multiple independent experiments. d, days.

weight (Fig. 2A) (P value of <0.0001 compared to the ECTV wt) nor showed any signs of illness (data not shown) throughout the period of observation. These data confirm N1 as a virulence factor in ECTV.

To determine the degree of attenuation, we infected mice intranasally with increasing doses of ECTVΔN1L. The 10-fold-higher dose of 2,000 PFU caused disease progression paralleling that of mice infected with the ECTV wt up to day 8 p.i., characterized by incipient weight loss, before all animals started to recover (Fig. 2C and D). When a dose of 20,000 PFU was applied, ECTVΔN1L elicited severe disease, and five out of six mice died, with an MTTD of 8.6 days (Fig. 2D). Interestingly, animals started to lose weight 2 days earlier than ECTV wt-infected animals, i.e., at day 4 p.i. (Fig. 2C). This effect was even more pronounced in mice infected with 200,000 PFU of ECTVΔN1L, the highest dose tested. Animals started to lose weight yet another day earlier, i.e., at day 3 p.i. (Fig. 2C), and all mice had already succumbed to the infection by day 9 p.i. (Fig. 2D) (MTTD of 8 days). Thus, ECTVΔN1L is highly attenuated, up to 100-fold, in this infection model.

ECTVΔN1L *in vivo* spreading is blocked in the lung early after infection. As described by Fenner (23), following initial replication at the site of infection, ECTV is systemically distributed to internal organs such as the liver and spleen. Upon respiratory infection, ECTV is expected to be transmitted first from the lung to the draining lymph nodes (mediastinal lymph nodes) and from there via the bloodstream to the spleen and liver. Since a spreading deficiency due to deletion of single genes was previously shown to be associated with attenuation (15, 16, 43, 60), we investigated the ability of ECTVΔN1L to

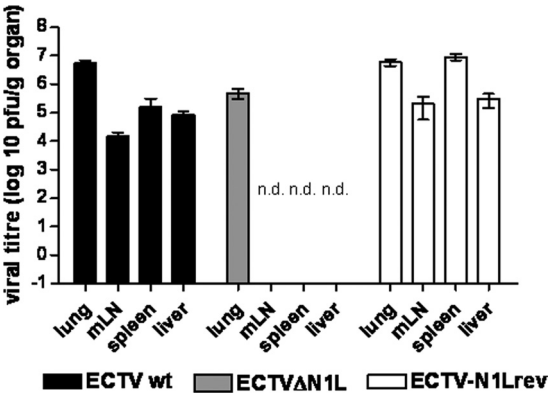

FIG. 3. Analysis of viral load in different organs after intranasal infection of C57BL/6 mice. C57BL/6 mice were infected with 200 PFU of the ECTV wt, ECTVΔN1L, or ECTV-N1Lrev, respectively (three animals per group). At day 6 p.i., the lung, mediastinal lymph nodes (mLN), spleen, and liver were removed and homogenized, and the amount of virus was determined by plaque assay. Data are representative of results of two independent experiments. n.d., not detectable.

spread to various target organs. We intranasally infected mice with 200 PFU of the ECTV wt, ECTVΔN1L, or ECTV-N1Lrev and determined viral loads in the lung, mediastinal lymph nodes, spleen, and liver on day 6 p.i. (Fig. 3). In the lungs of mice with all three viruses, we found high titers of infectivity (ranging from approximately 5×10^5 to 6×10^6 PFU/g of organ), with ECTVΔN1L producing slightly reduced levels of virus in comparison to those made by ECTV wt or ECTV-N1Lrev. Upon infection with the ECTV wt or ECTV-N1Lrev, which are fully virulent viruses, we also determined that there were substantial virus titers for lymph node, spleen, and liver tissues (ranging from 1×10^4 to 8×10^6 PFU/g of organ). Yet strikingly, we failed to detect ECTVΔN1L in any tissue other than that of the lung, indicating that the *in vivo* spread of this mutant virus was readily blocked at the site of the primary infection.

Notably, histopathologic examination of tissue from the sacrificed mice confirmed the virus load data from organ samples (Fig. 4). At day 6 p.i., necrotic lesions in the epithelia of lung bronchioles were visible upon infection with all viruses, including the mutant virus ECTVΔN1L (Fig. 4B to D). In contrast, hepatic lesions, consisting of focal necrosis, were detectable only for ECTV wt- or ECTV-N1Lrev-infected animals (Fig. 4F and H) and not in the livers of mice infected with ECTVΔN1L (Fig. 4G), further corroborating a spreading defect for ECTVΔN1L.

To investigate the kinetics and extent of viral *in vivo* replication and spread in more detail, mice were again infected with 200 PFU of the ECTV wt or ECTVΔN1L, and the viral load in the lung, liver, and spleen was analyzed on days 0, 3, 6, and 9 p.i. (Fig. 5). In the lungs of mice infected with ECTV wt, infectivity was already detectable 3 days p.i., with titers steadily increasing to approximately 5×10^6 PFU/g of organ on day 9 p.i. (Fig. 5A), indicating massive replication of the virus in lung tissue. In the spleen of one animal, virus was detected as early as day 3 p.i. (Fig. 5C), and all animals exhibited virus loads in both the liver and spleen 6 days p.i., with respective average titers of 2×10^4 PFU/g of organ and 1×10^5 PFU/g of organ (Fig. 5B and C). Later, at day 9 p.i., virus titers decreased minimally, by about half a log step, in the liver (Fig. 5B) and by approximately one log step in the spleen (Fig. 5C). Similarly, virus replication was also detectable in the lungs of ECTVΔN1L-infected mice, although titers again seemed in general slightly lower than those with the ECTV wt (Fig. 3 and 5A) at the same infectious dose. Following an initial titer of 1×10^3 PFU/g of organ on day 3 p.i. (*P* value of 0.0049 compared to ECTV wt), the virus load peaked at day 6 p.i. ($\sim 5 \times 10^4$ PFU/g of organ, *P* value of 0.0011) and decreased again on day 9 p.i. (Fig. 5A) (*P* value of <0.0001). Importantly, ECTVΔN1L was not detected in either the liver or spleen at any time point analyzed (Fig. 5B and C). Since increasing the infectious dose restored ECTVΔN1L pathogenicity in mice (Fig. 2C and D), we next examined if such high doses would enable mutant virus spread. As expected, mice infected with 2,000 PFU or 20,000 PFU of ECTVΔN1L showed an increased viral load in the lungs at day 3 p.i., comparable to that observed with the lungs of ECTV wt-infected mice (Fig. 5A) (*P* values of 0.9871 and 0.2908 compared to the ECTV wt, respectively). At day 6 p.i., viral titers increased to approximately 3×10^5 PFU/g of organ or 7×10^6 PFU/g of organ, respectively, following inoculation with 2,000 PFU (*P* value of 0.1720) or 20,000 PFU (*P* value of 0.0139) of ECTVΔN1L. However, viral titers of mice infected with 2,000 PFU declined again on day 9 p.i. (*P* value of 0.0065), as observed for mice infected with 200 PFU. Viral load was not determined on day 9 p.i. in animals infected with 20,000 PFU, since our previous experiment had shown that most mice die beforehand (MTTD of 8.6 days) (Fig. 2C). Remarkably, for both doses, mutant virus infectivity was again not detected in the liver or in the spleen at any time point (Fig. 5B and C). Apparently, ECTVΔN1L was unable to spread from the lung, regardless of the infectious dose applied.

Control of ECTVΔN1L infection is independent of TLR and RLH signaling. To elucidate if control of ECTVΔN1L infection was mediated by early immune sensing and signaling, we investigated the impact of pattern recognition receptors (PRRs), such as Toll-like receptors (TLRs) and RIG-I-like RNA helicases (RLHs) (68), on ECTVΔN1L pathogenicity. Within the cell, TLR signals are transmitted via the adaptor molecules myeloid differentiation primary response gene 88 (MyD88) and TIR-domain-containing molecule 1 (TRIF), either alone or in combination, whereas intracellular RLH signaling is mediated by Cardif (CARD adaptor inducing beta interferon [IFN-β]; also known as IPS-1) (68).

Groups of MyD88$^{-/-}$ TRIF$^{-/-}$ or Cardif$^{-/-}$ mice were infected intranasally according to our standard protocol. While ECTV wt infection induced weight loss and death in both knockout mouse strains (MTTD of 8 or 11.7 days), all mice infected with ECTVΔN1L survived, showing neither weight loss nor signs of illness throughout the period of investigation (Fig. 6A and B) (*P* values of <0.0001 and 0.0257, respectively, compared to the ECTV wt). These data suggest that TLR and RLH signaling pathways do not contribute to the control of ECTVΔN1L infection.

Another important part of the early immune reaction to viral infections are type I IFNs, which are sensed via the common IFN-α/β receptor (IFNAR). Since mice deficient in this receptor are unable to respond to type I IFNs (52), they were used to assess the contribution of type I IFNs. Infection of

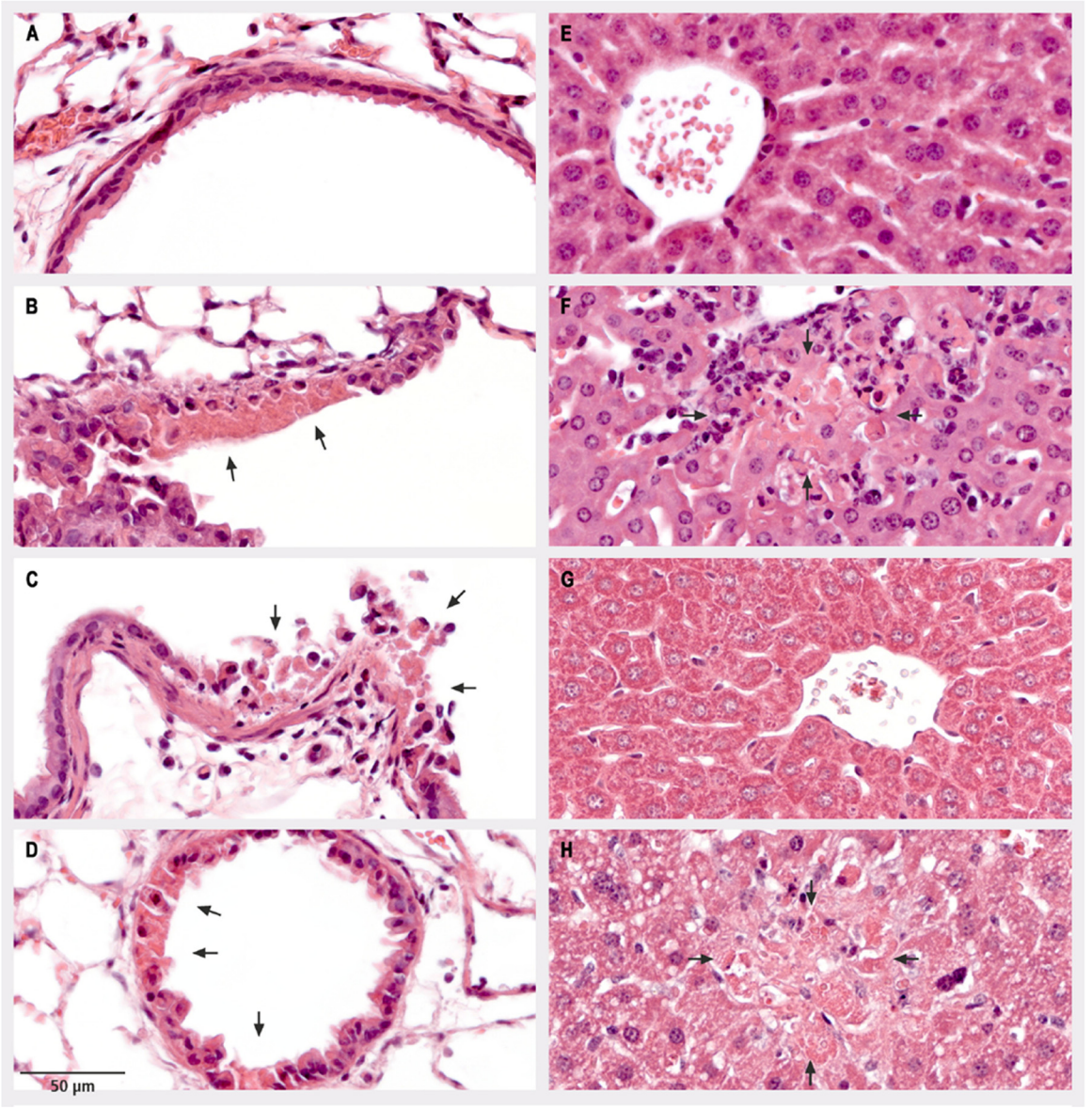

FIG. 4. Histopathologic analysis of lung and liver tissues from C57BL/6 mice. C57BL/6 mice were mock infected (A and E) or infected intranasally with 200 PFU of the ECTV wt (B and F), ECTVΔN1L (C and G), or ECTV-N1Lrev (D and H). On day 6 p.i., thin sections of lung (A to D) and liver (E to H) tissues were prepared and subjected to staining with hematoxylin and eosin. Arrows indicate focal acute necrosis of epithelial cells of the bronchiolus (B, C, and D) and focal necrosis of hepatocytes (F and H).

IFNAR$^{-/-}$ mice with the ECTV wt induced rapid weight loss and mortality with an MTTD of 7.5 days (Fig. 6C) (P value, <0.0001 compared to the control), comparable to results with MyD88$^{-/-}$ TRIF$^{-/-}$ mice. However, in contrast to results with MyD88$^{-/-}$ TRIF$^{-/-}$ and Cardif$^{-/-}$ mice, ECTVΔN1L infection evoked a slight, but not significant increase in morbidity in IFNAR$^{-/-}$ mice (Fig. 6C) (P value, <0.0001 compared to ECTV wt, and 0.5302 compared to the control), suggesting that type I interferons marginally contribute to the control of ECTVΔN1L infection during the early stage of disease.

Adaptive immunity is necessary to control late ECTVΔN1L infection. Since the innate immune system did not seem to play a major role in controlling infection with ECTV lacking the N1L gene, we investigated the impact of the adaptive immune response. We therefore studied infection in RAG-1$^{-/-}$ mice deficient in mature B and T cells due to an inability to perform V(D)J recombination (50). Following infection with the wild-type virus, mice started to lose weight between day 5 and day 7 p.i., and all animals died by day 11 p.i. (Fig. 7A) (MTTD of 10.8 days). Surprisingly, disease development was also observed for these mice following ECTVΔN1L infection, resulting in the death of all animals. In contrast to ECTV wt infection in both C57BL/6 and RAG-1$^{-/-}$ mice, ECTVΔN1L infection did not take effect until day 16 p.i. in RAG-1$^{-/-}$ mice, followed by gradual weight loss (Fig. 7A) (P value, <0.0001) and slowly increasing signs of illness (data not shown). Finally, all animals succumbed to the infection by day 33 p.i., with an MTTD of 28.8 days, suggesting an important

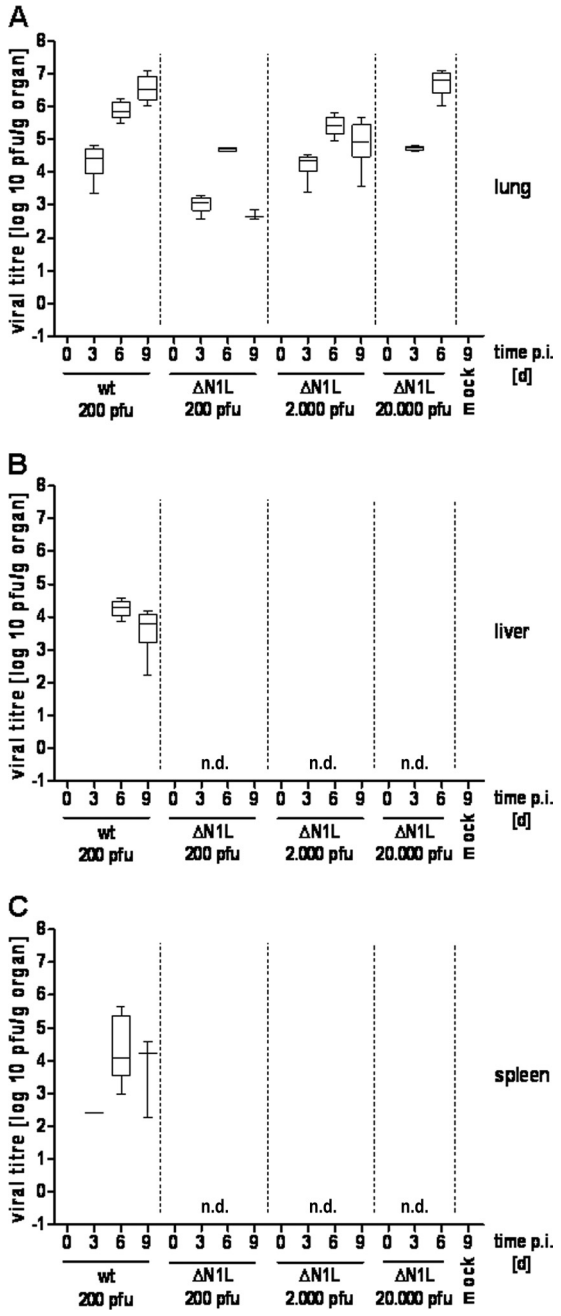

FIG. 5. Analysis of viral load in different organs after intranasal infection of C57BL/6 mice. C57BL/6 mice were mock infected (two animals) or infected with 200 PFU of the ECTV wt or with 200 PFU, 2,000 PFU, or 20,000 PFU of ECTVΔN1L (four animals per group). At the indicated time points p.i., the lung (A), liver (B) and spleen (C) were removed and homogenized, and the amount of virus was determined by plaque assays. Data are representative of results of two independent experiments. d, days; n.d., not detectable.

contribution of B and/or T cells in controlling ECTVΔN1L infection.

NK cells are important in controlling ECTV infection but do not significantly alter ECTVΔN1L infection. As shown before, adaptive immunity was essential to control ECTVΔN1L but seemed to affect only the late phase of infection. In order to define cell populations that might control the early phase of infection, we investigated the role of NK cells. As important components of the innate immune system, these cells are involved in resistance to many viral infections and are therefore also the target of numerous viral immune evasion strategies (36). To assess the role of NK cells, C57BL/6 mice were depleted of NK cells prior to infection. NK cell-depleted mice infected with the ECTV wt started to lose weight approximately 1 day earlier than their wild-type counterparts (MTTD of 8.8 days), which was not significant (*P* value, 1.0). However, NK cell depletion had no effect on ECTVΔN1L-infected animals, since they showed no weight loss (Fig. 7B) (*P* value of 0.0052 comparing NK cell-depleted ECTV wt and NK cell-depleted ECTVΔN1L).

However, due to the strong attenuation of ECTVΔN1L, any putative contribution of NK cells to controlling infection might not become apparent in wild-type C57BL/6 mice. Therefore, the impact of NK cells in RAG-$1^{-/-}$ mice analogously depleted of NK cells was investigated. Upon ECTVΔN1L infection, the overall delay in the onset of disease, as observed for nondepleted RAG-$1^{-/-}$ mice, was barely changed; only the disease progression in the absence of NK cells was altered, being slightly more pronounced. Weight loss in this group started approximately 1 to 2 days earlier, between day 12 and day 17 p.i. (Fig. 7C) (*P* value, 0.0030), and all animals had succumbed to infection by day 25 p.i., with an MTTD of 23.8 days. Since this shift toward an earlier onset of disease resembled results for ECTV wt-infected NK cell-depleted C57BL/6 mice (Fig. 7B), the contribution of NK cells seemed to be restricted to controlling ECTV infection in general, thus indicating that the attenuation of ECTV lacking the N1 protein is not due to NK cell function.

Lack of adaptive immunity allows spreading of ECTVΔN1L from the lung to the liver and spleen. The lethal course of ECTVΔN1L infection in RAG-$1^{-/-}$ mice posed the question of whether ECTVΔN1L was able to systemically spread in these mice lacking mature B and T cells. We analyzed the viral load in the lungs, livers, and spleens of RAG-$1^{-/-}$ and C57BL/6 mice, collecting organs when individual animals died due to infection or at the end of the experiment at day 32 p.i. (Fig. 8). The ECTV wt was readily detectable in organs of C57BL/6 mice that had succumbed to the infection, with titers in lung, liver, and spleen samples ranging from 7 to 16×10^5 PFU/g of tissue. In contrast, at day 32 following ECTVΔN1L infection, the virus was not detected in lung, liver, or spleen tissues of C57BL/6 mice, likely due to full virus clearance. Strikingly, however, with RAG-$1^{-/-}$ mice, we found high titers (2×10^6 PFU/g of tissue for the lung and spleen, up to about 1×10^8 PFU/g tissue in the liver) for ECTVΔN1L in all organs at the time of death (Fig. 8). These data suggested B and/or T cells as important effectors in controlling ECTVΔN1L spread. Furthermore, the ability of the ECTV wt to spread in the presence of these two cell populations (C57BL/6 mice) implied that N1 might interfere with B and/or T cell immune function.

Both $CD4^+$ and $CD8^+$ T cells are crucial components that contain ECTVΔN1L infection. In order to further elucidate whether B or T cells alone would be sufficient to control ECTVΔN1L infection, we investigated putative effects in JHT mice that are completely B cell deficient (29) and in mice with

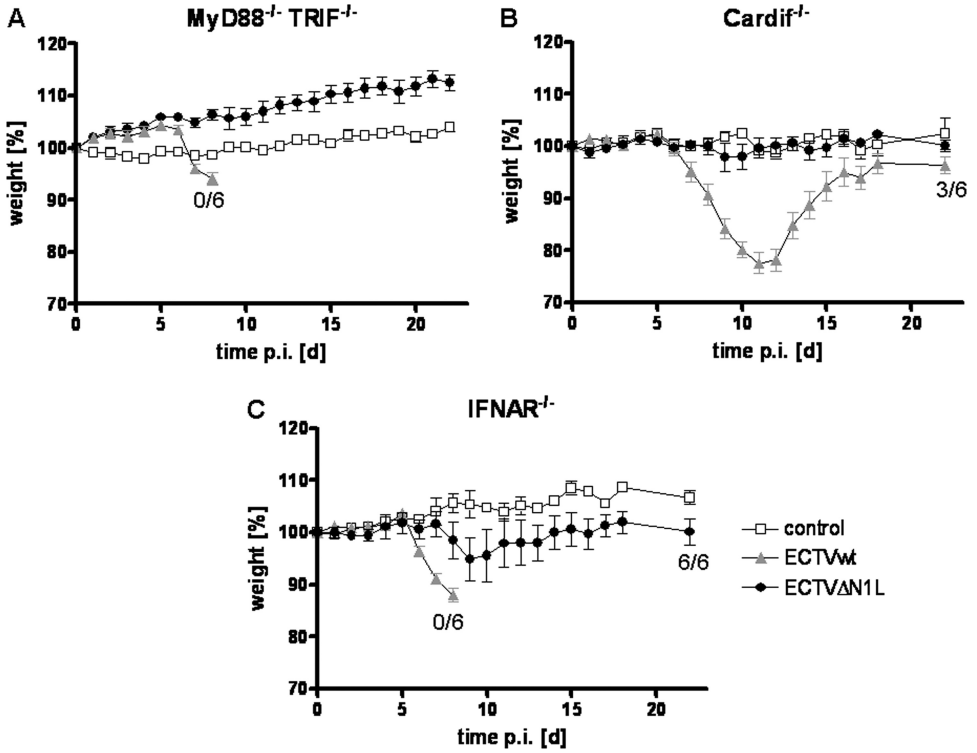

FIG. 6. Influence of TLR, RLH signaling, and type I interferons on the control of ECTVΔN1L infection in mice. MyD88$^{-/-}$ TRIF$^{-/-}$ (A), Cardif$^{-/-}$, (B) and IFNAR$^{-/-}$ (C) mice were mock infected (two or three animals per group) or infected intranasally with 200 PFU of the ECTV wt or ECTVΔN1L (five or six animals per group). Weight changes were recorded daily and are expressed as percent initial body weight. Additionally, the number of animals that survived the infection of the total number of animals per group is indicated where appropriate. Standard deviation is given as the SEM. d, days.

specific depletions of CD4$^+$ and CD8$^+$ T cell subsets. Interestingly, no weight loss or signs of illness were observed for JHT mice following ECTVΔN1L infection (Fig. 9A) (*P* value of <0.0001 compared to the ECTV wt; data not shown) throughout a 32-day period, indicating that B cells were not involved in the control of ECTVΔN1L infection. In sharp contrast, animals depleted of CD4$^+$ and CD8$^+$ T cells showed dramatic disease progression (Fig. 9D) (*P* value of <0.0001 compared to the ECTV wt) similar to that seen for RAG-1$^{-/-}$ mice (Fig. 6A). While after ECTV wt infection, mice started to lose weight from day 6 p.i. onward (MTTD of 9.7 days), mice infected with ECTVΔN1L did so starting around day 16 p.i., all succumbing to infection by day 29 p.i., with an MTTD of 26.2 days (*P* value of <0.0001 compared to the ECTV wt, *P* value of 0.0001 compared to the control). In animals with depletions of either CD4$^+$ or CD8$^+$ T cells, however, ECTVΔN1L infection did not elicit overt signs of morbidity, such as weight loss or signs of illness (Fig. 9B and C) (*P* value of <0.0001 compared to the ECTV wt). Thus, only removal of both T cell subsets allowed the N1L-deleted virus to regain virulence (Fig. 9B, C, and D). This emphasizes the sufficiency of either T cell population to maintain control of attenuated ECTVΔN1L infection in the respiratory mouse model.

DISCUSSION

As a natural mouse pathogen, ECTV offers the unique opportunity to study virus-host interactions within an evolutionarily adapted system. While orthopoxvirus gene functions have mostly been investigated using VACV, in particular the study of immunomodulatory genes and virulence factors could benefit tremendously from the native ECTV virus-host system. It is more likely to reveal new insights into gene functions that work primarily *in vivo*. In comparison to VACV, ECTV is genetically more closely related to VARV (30). Indeed, the similarity of ECTV and VARV extends beyond genetics, since both viruses are highly pathogenic, cause systemic infections in their respective hosts, and are characterized by a narrow host range (49). The mouse model of ECTV infection therefore provides an excellent *in vivo* model to understand VARV infection of humans, smallpox pathogenesis, and the pathogen's interaction with the host immune response.

Although the poxvirus regulatory protein N1 has been described as a strong virulence factor in VACV (3, 40), the underlying mechanisms are still unknown. We analyzed N1 function in the ECTV model system using a deletion mutant of the VACV N1L gene homolog (ECTVΔN1L, ORF 020). Attenuation of VACV mutants lacking N1L gene functions was shown for several mouse strains by different application routes (3, 33, 40, 48).

As early as 1949, Fenner suggested that the pathogenesis of mousepox after intranasal inoculation of small doses of virus resembles that of smallpox caused by VARV (25). Hence, we chose to investigate ECTV infection via the intranasal route in C57BL/6 mice, a system already known to induce severe dis-

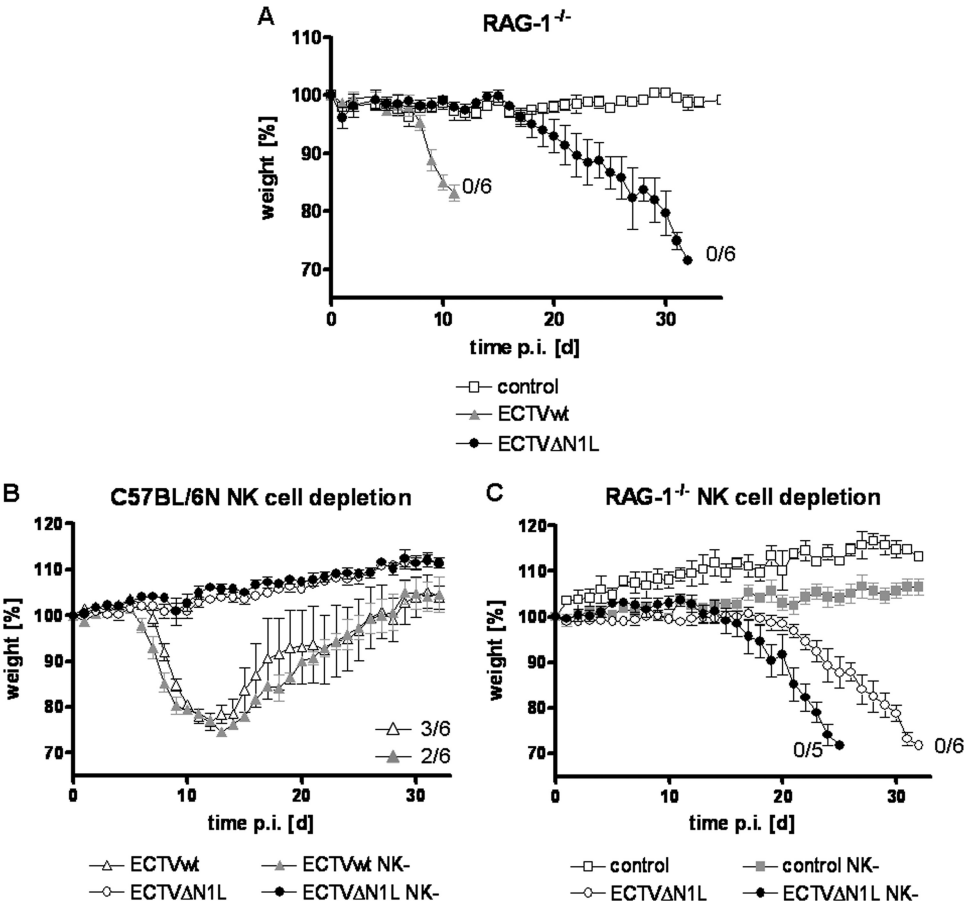

FIG. 7. Contribution of B, T, and NK cells to the control of ECTVΔN1L infection in mice. (A) Contribution of B and T cells to the control of ECTVΔN1L infection. Groups of five RAG-$1^{-/-}$ mice were mock infected or infected with 200 PFU of the ECTV wt or ECTVΔN1L. Weight, expressed as percent initial body weight, was monitored daily. The standard deviation is given as the SEM. (B) Contribution of NK cells to the control of ECTVΔN1L infection. C57BL/6 mice were depleted of NK cells using a specific monoclonal antibody and afterward mock infected (three animals per group) or infected with 200 PFU of the ECTV wt or ECTVΔN1L (six animals per group). Weight, expressed as percent initial body weight, was monitored daily. The standard deviation is given as the SEM. (C) RAG-$1^{-/-}$ mice were depleted of NK cells and afterward mock infected (three to four animals per group) or infected with 200 PFU of the ECTV wt or ECTVΔN1L (six animals per group). Weight, expressed as percent initial body weight, was monitored daily. The standard deviation is given as the SEM. For all curves, the number of animals that survived the infection of the total number of animals per group is indicated where appropriate. d, days.

ease with death at low virus doses (54). Our ECTVΔN1L derivative confirmed the previously described attenuation of N1L-deficient VACV mutants (3, 33, 40, 48). Whereas low doses of the ECTV wt were lethal, ECTVΔN1L did not induce any disease symptoms or even death until challenge doses were increased 10- or even 100-fold. Interestingly, the degree of ECTVΔN1L attenuation was similar to that described for VACV WR lacking N1L (48). Additionally, the high conservation of N1L among orthopoxviruses (3), with an amino acid identity ranging from approximately 89% (VACV Cop, ORF 032) to 92% (VARV BGD75maj, ORF 019), further highlights the importance of this virulence factor.

The most intriguing result of using the natural mouse model of ECTV infection to unravel the mechanisms of N1-mediated virulence was the inability of ECTVΔN1L to spread from the lung to the draining lymph node and to internal organs, such as the liver and spleen. Such a phenotype has not been observed before, highlighting it as a specific feature of ECTVΔN1L infection. Moreover, the spreading deficiency was not due to the low infectious dose, since increasing this 100-fold, which resulted in lethal respiratory infection, still did not enable virus dissemination from lung tissue. Mice infected with ECTVΔN1L at high doses apparently died from severe pneumonia, which also seems to be the cause of death in other orthopoxvirus infection models using harsh respiratory challenges (9, 25, 46, 48, 51, 61, 69).

Furthermore, the lack of ECTVΔN1L in the secondary target organs, the liver and spleen, was obviously not due to impaired virus replication. ECTVΔN1L multiplied in the mouse lung to levels equal to that for the ECTV wt, as was shown previously for VACVΔN1L (33, 48). Although ECTVΔN1L lung virus titers were lower than those of the ECTV wt 3 days p.i., they increased with the same magnitude over the next 3 days. Moreover, ECTVΔN1L was also able to replicate *in vitro* in murine NIH 3T3 cells (Fig. 1C), murine macrophages, lung alveolar epithelial cells, and even primary splenocytes to levels comparable to those of the ECTV wt (data not shown). Therefore, deletion of the N1L

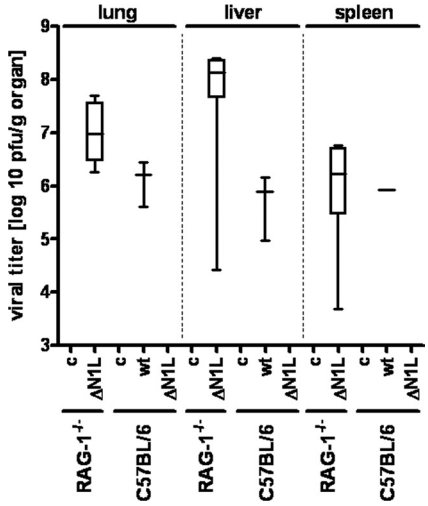

FIG. 8. Analysis of viral load in the liver, spleen, and lung tissues of RAG-$1^{-/-}$ and C57BL/6 mice. Organs of RAG-$1^{-/-}$ mice were collected when individual animals died due to infection, ranging from day 26 to day 32 p.i. for the group infected with ECTVΔN1L. The organs of control animals were removed at the end of the experiment (day 32 p.i.). C57BL/6 mice infected with the ECTV wt that succumbed to infection died between day 10 and day 14 p.i. All other C57BL/6 mice infected with the ECTV wt or ECTVΔN1L that did not die during the period of observation were sacrificed at the end of the experiment (day 32 p.i.), and organs were removed and homogenized. Viral titers were determined by plaque assays. c, control; ΔN1L, ECTVΔN1L; wt, ECTV wt.

ORF had not affected the ability of ECTV to replicate *in vitro* and *in vivo*.

These findings strongly suggest that other mechanisms are responsible for the absence of virus in spleen and liver. Following the initial increase in viral titers in the lung, the virus load of ECTVΔN1L decreased again between day 6 and day 9 p.i., in direct contrast to results for the ECTV wt. This suggests that the virus was cleared more rapidly and/or more efficiently from lung tissue by the immune system and that specific activation of the immune system permitted by the N1L deletion might play a role in the ECTVΔN1L virus's attenuation. In line with this, the histopathologic examination has provided the first indications of a more pronounced infiltration of immune cells into the lung following ECTVΔN1L infection (Fig. 4C). However, further studies are needed to address these initial observations in greater detail.

One of the important key molecules in immune activation is NF-κB, and N1L was implicated in inhibiting NF-κB function by interfering at the level of the IKK complex (18). Moreover, one NF-κB-activating stimulus, TLR9, was reported to be essential for survival of a lethal poxvirus infection in mice (58). However, ECTVΔN1L did not induce any disease symptoms in mice deficient in TLR signaling pathways (MyD88$^{-/-}$ TRIF$^{-/-}$ mice lacking both adaptor molecules), indicating that sensing by these pattern recognition receptors was not involved in the control of ECTVΔN1L infection. Likewise, RLH signaling by the intracellular double-stranded RNA (dsRNA) sensors MDA-5 and RIG-I (68) did not contribute to controlling ECTVΔN1L infection, given that respiratory infection of Cardif$^{-/-}$ mice remained asymptomatic. In terms of selected innate immune defenses, only type I interferons were apparently able to influence the outcome of infection, since ECTVΔN1L elicited some degree of morbidity in IFNAR$^{-/-}$ mice.

Numerous reports highlight the importance of single components of the innate immune system, especially Toll-like receptors and type I interferons, in surviving or recovering from an ECTV infection (38, 58). Indeed, the more rapid morbidity and mortality observed upon ECTV wt infection of the knockout mice (MyD88$^{-/-}$ TRIF$^{-/-}$, Cardif$^{-/-}$, and IFNAR$^{-/-}$) emphasized the overall importance of these components in the host's immune response to ECTV infection. However, the essential requirement for TLR or RLH signaling ceased in the absence of the N1 protein. This phenotype requires closer investigation, perhaps by increasing infectious doses in IFNAR$^{-/-}$ mice or analyzing the possible need for other newly identified immune sensors.

In this regard, the cytosolic DNA sensor DNA-dependent activator of IFN regulatory factor (DAI) plays an important role in the DNA-mediated activation of the innate immune system (67). Upon DNA binding, DAI oligomers or multimers form and subsequently recruit the serine/threonine kinase TBK1 (TANK-binding kinase 1) and the transcription factor interferon regulatory factor 3 (IRF3) into a complex (67, 71). When the activated IRF3 then translocates into the nucleus, the transcription of the type I interferons IFN-α and -β, among other responsive genes, is induced (71). Since a putative interaction of the VACV N1 protein with TBK1 has already been described (18), DAI might be a good candidate for further investigation.

In addition, the absent in melanoma 2–apoptosis-associated speck-like protein containing CARD-1 (AIM2-ASC) pathway has been reported to play a critical role in innate immune responses to DNA viruses (31, 56). It was shown that infection of bone marrow-derived macrophages (BMDMs) or bone marrow-derived dendritic cells (BMDCs) of *Aim2*$^{+/+}$ mice with VACV stimulated the release of mature IL-1β into the supernatant and the cleavage of caspase-1. However, this response was attenuated in BMDMs and BMDCs of *Aim2*$^{-/-}$ mice (56).

Recently, CD103^{+} DCs were shown to be highly effective antigen-presenting cells for the activation of naïve CD8^{+} T cells following a respiratory VACV infection. Upon infection or acquisition of viral antigen, these cells traffic to the draining lymph node, where they potentially serve as activators of naïve T cells, inducing proliferation and acquisition of effector functions (4). As these processes would critically affect any intranasal infection, the involvement of CD103^{+} DCs in the control of ECTVΔN1L infection should be addressed in future studies.

Significantly, restoration of the spreading capacity of ECTVΔN1L in RAG-$1^{-/-}$ mice strongly implied that adaptive immunity contributes to the control of virus infection. In line with this, a previous study described the induction of a robust T cell immune response after intranasal infection with VACVΔN1L (48). However, Jacobs and colleagues attributed the attenuated phenotype of the VACV N1L deletion mutant virus to increased transient NK cell influx into the infected tissue and enhanced NK cell activity after intradermal application (33). Since several studies have already stressed the importance of the NK cell population in ECTV infection (22, 34, 55), we analyzed their involvement in controlling ECTVΔN1L infection in NK cell-depleted mice. In our respi-

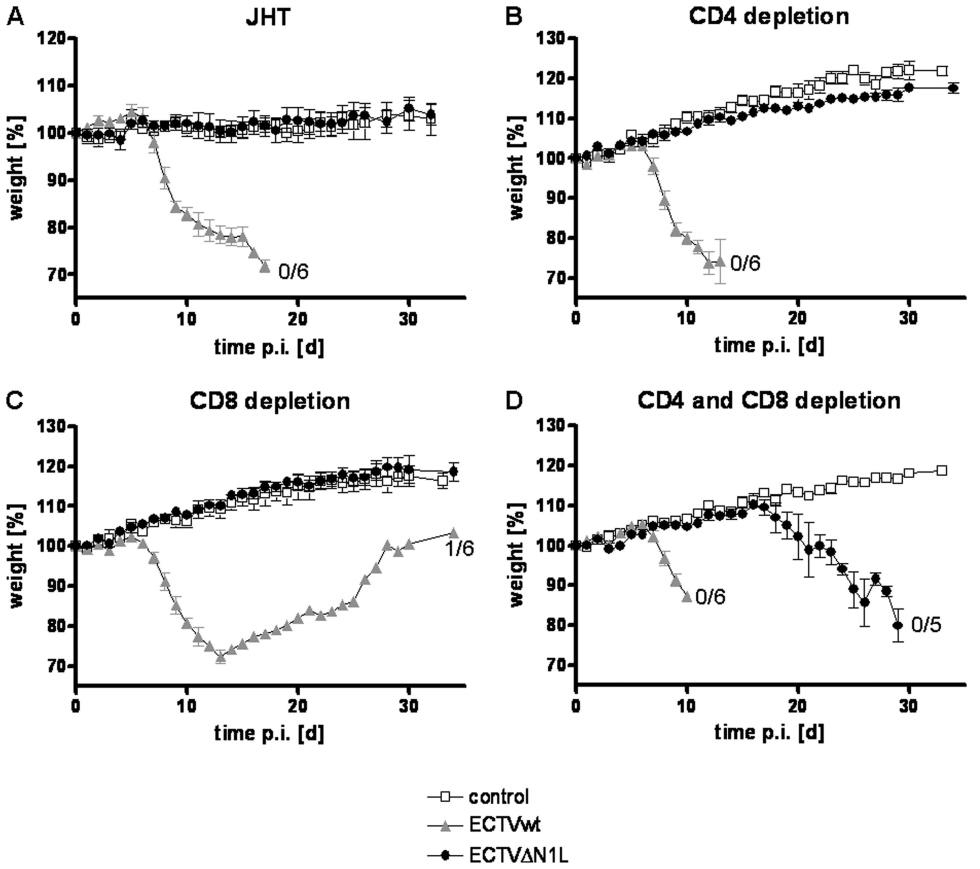

FIG. 9. Contribution of B and T cells to the control of ECTVΔN1L infection. (A) JHT mice were mock infected (four animals per group) or infected with 200 PFU of the ECTV wt or ECTVΔN1L (six animals per group). The body weight was recorded daily and is shown as percent initial body weight. The standard deviation is given as the SEM. (B to D) C57BL/6 mice were depleted of $CD4^+$ (B), $CD8^+$ (C), or $CD4^+$ and $CD8^+$ T (D) cells using specific monoclonal antibodies. Afterward, mice were infected with 200 PFU of the ECTV wt or ECTVΔN1L (six animals per group) or were mock infected (three animals per group). The body weight, expressed as percent initial body weight, was monitored and recorded daily. The standard deviation is given as the SEM. For all curves, the number of animals that survived the infection of the total number of animals per group is indicated where appropriate. d, days.

ratory mousepox model, we could not confirm a contribution of NK cells to ECTVΔN1L clearance. Furthermore, depletion of NK cells induced the same disease-onset shift in ECTVΔN1L-infected B and T cell-deficient RAG-$1^{-/-}$ mice as in ECTV wt-infected C57BL/6 mice. This finding suggests that NK cells facilitate control of ECTV infection in general, but irrespectively of N1 function.

Previous studies have accentuated the importance of B and T cells in surviving and recovering from an ECTV infection (12, 37, 53). In agreement, our analysis of ECTVΔN1L infection in RAG-$1^{-/-}$ mice demonstrated a clear dependency on adaptive immunity to control infection. Also in line with these observations was the high mortality rate of ECTV wt-infected JHT mice, which are deficient in functional B cells (29), as well as the recurrence of typical pock lesions in surviving mice (data not shown).

In clear contrast, infection of these mice with ECTV lacking the VACV N1L homolog did not elicit any morbidity, indicating that neither B cells nor antibodies were important for clearance of this mutant virus. Instead, we found that T cells are the key players controlling ECTVΔN1L infection. Depletion of only one subset, either $CD4^+$ or $CD8^+$ T cells, did not elicit morbidity or mortality upon ECTVΔN1L infection, but depletion of both T cell populations did, revealing that either the $CD4^+$ or the $CD8^+$ T cell subset was already sufficient for virus control.

A previous study attributed distinct roles to $CD4^+$ and $CD8^+$ T cells in control of an ECTV infection (37). Thymectomized C57BL/6 mice specifically depleted of either $CD8^+$ or $CD4^+$ plus $CD8^+$ T lymphocytes and inoculated with ECTV wt by the footpad route showed 100% mortality. On the other hand, all animals depleted of $CD4^+$ T lymphocytes survived infection, although they developed pock lesions later on. Furthermore, β2-$m^{-/-}$ mice, which lack mature $CD8^+$ T cells (39, 74), also succumbed to infection. Thus, the control of an ECTV wt infection relied on $CD8^+$ T cells (37). In our studies, ECTVΔN1L infection control was maintained in the presence of either the $CD4^+$ or the $CD8^+$ cell population, a finding in clear contrast to the ECTV wt infection that neither the $CD4^+$ nor $CD8^+$ T cell population alone could control. This discrepancy might be due to the different routes of application, and therefore different tissues infected, as route-dependent effects have been observed before (5).

ECTVΔN1L was clearly blocked in the lung at the site of

primary infection, since we failed to detect infectious virus in the draining lymph nodes (Fig. 3). Thus, we hypothesize that an efficient immune response in the lung can control the replication and prevent the spread of the mutant virus. Interestingly, in comparison to ECTV wt or ECTV-N1Lrev, the intranasal infection with ECTVΔN1L appeared to elicit a more pronounced peribronchiolar infiltrate of macrophages, neutrophils, and lymphocytes (Fig. 4C), supporting a putatively more efficient immune response in the absence of N1. However, a more detailed analysis will be needed for a thorough comparative characterization of lung-associated immune reactions in response to ECTVΔN1L infection.

In the context of respiratory infections of mice with vesicular stomatitis virus or *Listeria monocytogenes*, the lung has been shown to serve as a key nonlymphoid organ for homing and differentiation of effector T cells, enabling rapid containment of the pathogen (47). However, in the case of ECTVΔN1L infection, it remains to be determined if short-lived, virus-specific $CD8^+$ T cells also efficiently migrate to the lung and display immediate effector function. Interestingly, half of the ECTVΔN1L-infected C57BL/6 mice in our experiments depleted solely of $CD4^+$ T cells eventually developed pock lesions on their tails and feet (data not shown). This underscored the requirement for $CD4^+$ T helper cells, and thus B cells and antibodies, for complete virus clearance, as reported previously (37), although the presence of $CD4^+$ T helper cells might not be a prerequisite for the initial control of infection.

Whereas control of ECTVΔN1L at later time points of infection was attributed to T cells, the key players in immediate surveillance, i.e., those which control ECTVΔN1L infection and spreading during the first hours and days after infection, remain elusive. Nevertheless, our findings suggest that one role of the N1 protein is to impair T cell function. Taking into account that the N1 protein has been reported to inhibit the induction of apoptosis as well as NF-κB signaling (14, 18), it is possible that ECTVΔN1L-related pathogen-associated molecular patterns (PAMPs) and antigens are more efficiently recognized and processed by antigen-presenting cells. Likewise, in the absence of the N1 protein, unimpaired NF-κB signaling could lead to a more robust cytokine and chemokine expression, which may be important in shaping the adaptive immune response (e.g., in driving $CD4^+$ T cells toward a Th1 or Th2 fate). In consequence, these processes might together enhance, support, and/or aid T cell function and, ultimately, enable control of ECTVΔN1L infection.

In summary, we confirmed that the poxvirus regulatory protein N1 is a strong virulence factor by analyzing its function in ECTV, a natural mouse pathogen. The protein clearly contributed to virus spreading from the lung to further target organs after intranasal infection, obviously by interfering with functions of the adaptive immune system. However, the means by which it exerts this function remain to be determined in future studies. Furthermore, depletion of neither $CD4^+$ nor $CD8^+$ T cells alone could restore ECTVΔN1L virulence; thus, either T cell subset is essential and sufficient to control ECTVΔN1L infection. Possibly, these cells are also the key players controlling virus spread. Therefore, these data suggest that the N1 protein might, either directly or indirectly, interfere with T cell function to enable virus spreading.

ACKNOWLEDGMENTS

We thank Dorothea Kreuz for excellent support in mouse breeding and for providing the knockout mice for our experiments, Astrid Freudenstein for expert technical assistance, and Ulrike Mettler for helpful discussions.

This work was supported by grants from the European Commission (Biosafe SSPE-CT-2006-022725, MVACTOR LHSP-CT-2006-037536).

The authors declare no conflicts of interest.

REFERENCES

1. **Alcami, A.** 2003. Viral mimicry of cytokines, chemokines and their receptors. Nat. Rev. Immunol. **3:**36–50.
2. **Aoyagi, M., et al.** 2007. Vaccinia virus N1L protein resembles a B cell lymphoma-2 (Bcl-2) family protein. Protein Sci. **16:**118–124.
3. **Bartlett, N., J. A. Symons, D. C. Tscharke, and G. L. Smith.** 2002. The vaccinia virus N1L protein is an intracellular homodimer that promotes virulence. J. Gen. Virol. **83:**1965–1976.
4. **Beauchamp, N. M., R. Y. Busick, and M. A. Alexander-Miller.** 2010. Functional divergence among $CD103^+$ dendritic cell subpopulations following pulmonary poxvirus infection. J. Virol. **84:**10191–10199.
5. **Bivas-Benita, M., et al.** 2010. Efficient generation of mucosal and systemic antigen-specific $CD8^+$ T cell responses following pulmonary DNA immunization. J. Virol. **84:**5764–5774.
6. **Born, T. L., et al.** 2000. A poxvirus protein that binds to and inactivates IL-18, and inhibits NK cell response. J. Immunol. **164:**3246–3254.
7. **Bowie, A., et al.** 2000. A46R and A52R from vaccinia virus are antagonists of host IL-1 and toll-like receptor signaling. Proc. Natl. Acad. Sci. U. S. A. **97:**10162–10167.
8. **Boyle, D. B., and B. E. H. Coupar.** 1988. A dominant selectable marker for the construction of recombinant poxviruses. Gene **65:**123–128.
9. **Bray, M., et al.** 2000. Cidofovir protects mice against lethal aerosol or intranasal cowpox virus challenge. J. Infect. Dis. **181:**10–19.
10. **Breman, J. G., and D. A. Henderson.** 2002. Diagnosis and management of smallpox. N. Engl. J. Med. **346:**1300–1308.
11. **Brick, D. J., R. D. Burke, A. A. Minkley, and C. Upton.** 2000. Ectromelia virus virulence factor p28 acts upstream of caspase-3 in response to UV light-induced apoptosis. J. Gen. Virol. **81:**1087–1097.
12. **Chaudhri, G., V. Panchanathan, H. Bluethmann, and G. Karupiah.** 2006. Obligatory requirement for antibody in recovery from a primary poxvirus infection. J. Virol. **80:**6339–6344.
13. **Chen, N., R. M. Buller, E. M. Wall, and C. Upton.** 2000. Analysis of host response modifier ORFs of ectromelia virus, the causative agent of mousepox. Virus Res. **66:**155–173.
14. **Cooray, S., et al.** 2007. Functional and structural studies of the vaccinia virus virulence factor N1 reveal a Bcl-2-like anti-apoptotic protein. J. Gen. Virol. **88:**1656–1666.
15. **Cordeiro, J., et al.** 2009. F11-mediated inhibition of RhoA signalling enhances the spread of vaccinia virus in vitro and in vivo in an intranasal mouse model of infection. PLoS One **4:**e8506.
16. **Dénes, B., et al.** 2006. Attenuation of a vaccine strain of vaccinia virus via inactivation of interferon viroceptor. J. Gene Med. **8:**814–823.
17. **Di Giulio, D. B., and P. B. Eckburg.** 2004. Human monkeypox: an emerging zoonosis. Lancet Infect. Dis. **4:**15–25.
18. **DiPerna, G., et al.** 2004. Poxvirus protein N1L targets the I-κB kinase complex, inhibits signaling to NF-κB by the tumor necrosis factor superfamily of receptors, and inhibits NF-κB and IRF3 signaling by Toll-like receptors. J. Biol. Chem. **279:**36570–36578.
19. **Essbauer, S., M. Pfeffer, and H. Meyer.** 2010. Zoonotic poxviruses. Vet. Microbiol. **140:**229–236.
20. **Esteban, D. J., and R. M. Buller.** 2005. Ectromelia virus: the causative agent of mousepox. J. Gen. Virol. **86:**2645–2659.
21. **Falkner, F. G., and B. Moss.** 1990. Transient dominant selection of recombinant vaccinia viruses. J. Virol. **64:**3108–3111.
22. **Fang, M., L. L. Lanier, and L. J. Sigal.** 2008. A role for NKG2D in NK cell-mediated resistance to poxvirus disease. PLoS Pathog. **4:**e30.
23. **Fenner, F.** 1948. The clinical features and pathogenesis of mouse-pox (infectious ectromelia of mice). J. Pathol. Bacteriol. **60:**529–552.
24. **Fenner, F., D. A. Henderson, I. Arita, Z. Jezek, and I. D. Ladnyi.** 1988. Smallpox and its eradication. World Health Organization, Geneva, Switzerland.
25. **Fenner, F.** 1949. Mouse-pox (infectious ectromelia of mice): a review. J. Immunol. **63:**341–373.
26. **Finlay, B. B., and G. McFadden.** 2006. Anti-immunology: evasion of the host immune system by bacterial and viral pathogens. Cell **124:**767–782.
27. **Fischer, S. F., et al.** 2006. Modified vaccinia virus Ankara protein F1L is a novel BH3-domain-binding protein and acts together with the early viral protein E3L to block virus-associated apoptosis. Cell Death Differ. **13:**109–118.
28. **Garcia, M. A., S. Guerra, J. Gil, V. Jimenez, and M. Esteban.** 2002. Anti-

apoptotic and oncogenic properties of the dsRNA-binding protein of vaccinia virus, E3L. Oncogene **21:**8379–8387.
29. **Gu, H., Y. R. Zou, and K. Rajewsky.** 1993. Independent control of immunoglobulin switch recombination at individual switch regions evidenced through Cre-loxP-mediated gene targeting. Cell **73:**1155–1164.
30. **Gubser, C., S. Hue, P. Kellam, and G. L. Smith.** 2004. Poxvirus genomes: a phylogenetic analysis. J. Gen. Virol. **85:**105–117.
31. **Hornung, V., et al.** 2009. AIM2 recognizes cytosolic dsDNA and forms a caspase-1-activating inflammasome with ASC. Nature **458:**514–518.
32. **Horton, R. M., H. D. Hunt, S. N. Ho, J. K. Pullen, and L. R. Pease.** 1989. Engineering hybrid genes without the use of restriction enzymes: gene splicing by overlap extension. Gene **77:**61–68.
33. **Jacobs, N., N. W. Bartlett, R. H. Clark, and G. L. Smith.** 2008. Vaccinia virus lacking the Bcl-2-like protein N1 induces a stronger natural killer cell response to infection. J. Gen. Virol. **89:**2877–2881.
34. **Jacoby, R. O., P. N. Bhatt, and D. G. Brownstein.** 1989. Evidence that NK cells and interferon are required for genetic resistance to lethal infection with ectromelia virus. Arch. Virol. **108:**49–58.
35. **Johnston, J. B., and G. McFadden.** 2003. Poxvirus immunomodulatory strategies: current perspectives. J. Virol. **77:**6093–6100.
36. **Jonjic, S., M. Babic, B. Polic, and A. Krmpotic.** 2008. Immune evasion of natural killer cells by viruses. Curr. Opin. Immunol. **20:**30–38.
37. **Karupiah, G., R. M. Buller, N. Van Rooijen, C. J. Duarte, and J. Chen.** 1996. Different roles for $CD4^+$ and $CD8^+$ T lymphocytes and macrophage subsets in the control of a generalized virus infection. J. Virol. **70:**8301–8309.
38. **Karupiah, G., T. N. Fredrickson, K. L. Holmes, L. H. Khairallah, and R. M. Buller.** 1993. Importance of interferons in recovery from mousepox. J. Virol. **67:**4214–4226.
39. **Koller, B. H., P. Marrack, J. W. Kappler, and O. Smithies.** 1990. Normal development of mice deficient in beta 2M, MHC class I proteins, and $CD8^+$ T cells. Science **248:**1227–1230.
40. **Kotwal, G. J., A. W. Hugin, and B. Moss.** 1989. Mapping and insertional mutagenesis of a vaccinia virus gene encoding a 13,800-Da secreted protein. Virology **171:**579–587.
41. **Kotwal, G. J., and M.-R. Abrahams.** 2004. Growing poxviruses and determining virus titer. Methods Mol. Biol. **269:**101–112.
42. **Kumar, H., et al.** 2006. Essential role of IPS-1 in innate immune responses against RNA viruses. J. Exp. Med. **203:**1795–1803.
43. **Legrand, F. A., et al.** 2004. Induction of potent humoral and cell-mediated immune responses by attenuated vaccinia virus vectors with deleted serpin genes. J. Virol. **78:**2770–2779.
44. **Loparev, V. N., et al.** 1998. A third distinct tumor necrosis factor receptor of orthopoxviruses. Proc. Natl. Acad. Sci. U. S. A. **95:**3786–3791.
45. **Lorenzo, M. M., I. Galindo, and R. Blasco.** 2004. Construction and isolation of recombinant vaccinia virus using genetic markers. Methods Mol. Biol. **269:**15–30.
46. **Martinez, M. J., M. P. Bray, and J. W. Huggins.** 2000. A mouse model of aerosol-transmitted orthopoxviral disease. Arch. Pathol. Lab. Med. **124:**362–377.
47. **Masopust, D., V. Vezys, A. L. Marzo, and L. Lefrancois.** 2001. Preferential localization of effector memory cells in nonlymphoid tissue. Science **291:**2413–2417.
48. **Mathew, A., et al.** 2008. Robust intrapulmonary CD8 T cell responses and protection with an attenuated N1L deleted vaccinia virus. PLoS One **3:**e3323.
49. **McFadden, G.** 2005. Poxvirus tropism. Nat. Rev. Microbiol. **3:**201–213.
50. **Mombaerts, P., et al.** 1992. RAG-1-deficient mice have no mature B and T lymphocytes. Cell **68:**869–877.
51. **Montasir, M., E. R. Rabin, and C. A. Phillips.** 1966. Vaccinia pneumonia in mice: a light and electron microscopic and viral assay study. Am. J. Pathol. **48:**877–895.
52. **Muller, U., et al.** 1994. Functional role of type I and type II interferons in antiviral defense. Science **264:**1918–1921.
53. **Panchanathan, V., G. Chaudhri, and G. Karupiah.** 2006. Protective immunity against secondary poxvirus infection is dependent on antibody but not on CD4 or CD8 T-cell function. J. Virol. **80:**6333–6338.
54. **Paran, N., et al.** 2009. Postexposure immunization with modified vaccinia virus Ankara or conventional Lister vaccine provides solid protection in a murine model of human smallpox. J. Infect. Dis. **199:**39–48.
55. **Parker, A. K., S. Parker, W. M. Yokoyama, J. A. Corbett, and R. M. Buller.** 2007. Induction of natural killer cell responses by ectromelia virus controls infection. J. Virol. **81:**4070–4079.
56. **Rathinam, V. A. K., et al.** 2010. The AIM2 inflammasome is essential for host defense against cytosolic bacteria and DNA viruses. Nat. Immunol. **11:**395–402.
57. **Rimoin, A. W., et al.** 2010. Major increase in human monkeypox incidence 30 years after smallpox vaccination campaigns cease in the Democratic Republic of Congo. Proc. Natl. Acad. Sci. U. S. A. **107:**16262–16267.
58. **Samuelsson, C., et al.** 2008. Survival of lethal poxvirus infection in mice depends on TLR9, and therapeutic vaccination provides protection. J. Clin. Invest. **118:**1776–1784.
59. **Seet, B. T., et al.** 2003. Poxviruses and immune evasion. Annu. Rev. Immunol. **21:**377–423.
60. **Senkevich, T. G., E. V. Koonin, and R. M. Buller.** 1994. A poxvirus protein with a RING zinc finger motif is of crucial importance for virulence. Virology **198:**118–128.
61. **Smee, D. F., K. W. Bailey, and R. W. Sidwell.** 2001. Treatment of lethal vaccinia virus respiratory infections in mice with cidofovir. Antivir. Chem. Chemother. **12:**71–76.
62. **Smith, G. L.** 1999. Vaccinia virus immune evasion. Immunol. Lett. **65:**55–62.
63. **Smith, G. L., J. A. Symons, A. Khanna, A. Vanderplasschen, and A. Alcami.** 1997. Vaccinia virus immune evasion. Immunol. Rev. **159:**137–154.
64. **Smith, V. P., and A. Alcami.** 2000. Expression of secreted cytokine and chemokine inhibitors by ectromelia virus. J. Virol. **74:**8460–8471.
65. **Staib, C., M. Löwel, V. Erfle, and G. Sutter.** 2003. Improved host range selection for recombinant modified vaccinia virus Ankara. Biotechniques **34:**694–696, 698, 700.
66. **Stanford, M. M., G. McFadden, G. Karupiah, and G. Chaudhri.** 2007. Immunopathogenesis of poxvirus infections: forecasting the impending storm. Immunol. Cell Biol. **85:**93–102.
67. **Takaoka, A., et al.** 2007. DAI (DLM-1/ZBP1) is a cytosolic DNA sensor and an activator of innate immune response. Nature **448:**501–505.
68. **Thompson, A. J., and S. A. Locarnini.** 2007. Toll-like receptors, RIG-I-like RNA helicases and the antiviral innate immune response. Immunol. Cell Biol. **85:**435–445.
69. **Thompson, J. P., P. C. Turner, A. N. Ali, B. C. Crenshaw, and R. W. Moyer.** 1993. The effects of serpin gene mutations on the distinctive pathobiology of cowpox and rabbitpox virus following intranasal inoculation of Balb/c mice. Virology **197:**328–338.
70. **Waibler, Z., et al.** 2007. Modified vaccinia virus Ankara induces Toll-like receptor-independent type I interferon responses. J. Virol. **81:**12102–12110.
71. **Wang, Z., et al.** 2008. Regulation of innate immune responses by DAI (DLM-1/ZBP1) and other DNA-sensing molecules. Proc. Natl. Acad. Sci. U. S. A. **105:**5477–5482.
72. **Wasilenko, S. T., T. L. Stewart, A. F. Meyers, and M. Barry.** 2003. Vaccinia virus encodes a previously uncharacterized mitochondrial-associated inhibitor of apoptosis. Proc. Natl. Acad. Sci. U. S. A. **100:**14345–14350.
73. **Yamamoto, M., et al.** 2003. Role of adaptor TRIF in the MyD88-independent toll-like receptor signaling pathway. Science **301:**640–643.
74. **Zijlstra, M., et al.** 1990. Beta 2-microglobulin deficient mice lack CD4-8^+ cytolytic T cells. Nature **344:**742–746.